E-DNA biosensors of M. tuberculosis based on nanostructured polypyrrole

Rabih Khoder, Hafsa Korri-Youssoufi

E-DNA biosensors of *M. tuberculosis* based on Nanostructured Polypyrrole

Rabih Khoder and Hafsa Korri-Youssoufi*

University Paris-Saclay, Univ Paris-Sud, UMR-CNRS 8182, ICMMO, ECBB, Bat 420 91405 Orsay France

Abstract:

The objective of this paper is to demonstrate the potential of nanostructured polypyrrole formed by template free as platform for amperometric detection of DNA. The nanowires of polypyrrole (nw-PPy) are formed through electrochemical polymerization and chemically modified by electrochemical oxidation of ethylene diamine or dendrimers PAMAM to obtain aminated surface. The DNA probe and ferrocenyl group, as redox reporter, were covalently linked to the surface of nw-PPy. The chemical structure of nanostructured platform was characterized through SEM, FT-IR and XPS and the electrochemical properties through cyclic voltammetry and electrochemical impedance spectroscopy (EIS). We show that the properties of nw-PPy such as, hydrophilic character and large surface area have large effect on the electronic properties. Thus, the electrochemical performance is increased compared to others nanomaterials considering the obtained value of the rate of electron transfer of 18 s^{-1}. These properties allow enhanced DNA sensing where detection limit of 0.36 atomolar without any amplification step. The biosensor can be applied in detection of genomic DNA of Mycobacterium tuberculosis and the mutated one which present the resistance to rifampicin and large selectivity was demonstrated. We believe that nw-PPy modified with redox marker is a promising platform for electrochemical biosensors and can be applied for various diagnosis prospects.

Keywords: Polypyrrole, Nanowire, DNA, Electrochemical, Detection, *M. tuberculosis*.

Introduction

A rapid, accurate, cost-effective of diagnostics of pathogenic and viral DNA biomarkers stills remains a challenge. The development of extremely sensitive, highly selective, simple, robust and yet inexpensive biosensing platforms appears thus essential for a wide range of applications, including not only clinical diagnostics [1] but also environmental monitoring [2]

and food safety testing [3]. The detection and identification of multi-resistant strains are raising therapeutic problems. Tuberculosis remains one of major global health problem worldwide. Despite the advent of antibiotics which have widely reduced mortality, antibiotic-resistant strains have now emerged. The ability to obtain sequence-specific genetic information about infectious pathogens and resistant stand remains of great importance. Most methods used for DNA detection for diagnosis are PCR[4] and Q-PCR [5]. Recently various strategies were developed for label free DNA detection, such as fluorescence [6], [7]. Even these methods are sensitive they are not adapted to point of care analysis system. Thus, electrochemical DNA (E-DNA) biosensors have recently found extensive applications in diagnosis as well as analysis. E-DNA biosensors usually composed of two basic components, a DNA recognition system and a transducer which is a device that converts the chemical response into electrical signals that can be detected by various detection approaches[8] [9]. Several E-DNA biosensors using transducers have been developed for real time detection without amplification step. They include conducting materials [10] able to change their electrical properties after such hybridization reaction on their surface.

Conducting polymers (CPs) are widely used as transducers for biological interactions. CPs are π conjugated polymers with an electronic structure giving them intrinsic characteristics such as electrical conductivity, which can be controlled by a doping/de-doping process, low ionization potential, high electron transfer ability and optical properties. Polypyrrole (CPPy) is one of the conducting polymers extensively applied for the design of bioanalytical sensors [11] [12] including DNA detection [13]. This is related to their electrical, electrochemical properties as well as their ability of immobilization onto micro size surface by electropolymerisation [14]. One of their potential powerful is their ability for chemical modification and introduction of functional group that has a great's importance in the construction of biosensors devices [15]. E- DNA hybridization sensing based on CPPy has been achieved by measuring their electrical properties through impedance [16], amperometric [17] or redox markers [18]. Numerous publications concerning E-DNA biosensors based on CPPy with various approaches were developed. For example, molecular imprinted PPy [19], association of PPy with graphene [20] or with carbon nanotube [21] were shown to improve the detection performance. However, CPPy nanostructures present a greats interest in biosensors devices as these nanomaterials present high surface area comparable to carbon nanotubes, with tunable conductivity, flexibility, chemical diversity and easy processing [22]. Current research showed that vertically aligned PPy nanowires exhibit a unique combination

of morphology and intrinsic properties, such as high surface to volume ratio, fast oxidation/reduction kinetic and electrical conductivity [23].

nw-PPy can be obtained by a number of ways including growing on templates of inorganic materials such as anodic aluminium oxide [24] (AAO) membranes, zinc oxide [25] or template with organic materials such as, gelatin as soft mold [26]. The nanostructures of polypyrrole could also be formed through the nanotechnology approaches, through nanocontact printing and controlled polymerization [27]. Template free method of synthesizing nanostructures of CPPy has several advantages, like simple synthesis with no template removing steps needed. In addition, uniform and reproducible nanostructures are formed [28]. Various nanostructures could be formed within direct electropolymerization of pyrrole on electrode, depending on chemical and electrochemical conditions of use. For example, spherical PPy nanoparticles could be formed using potential pulses [29] where the size could be controlled [30]. nw-PPy without template has been demonstrated in the presence of non-acidic and week-acidic anions by the electropolymerization at fixed potential [31], where the length of the wire could be controlled [32]. Various electrochemical sensors based on nw-PPy have been presented for detection of small molecules such as NO_3^- ions [33], Cu^{2+} [34], ammonia gas [35], glutamic acid [36], spermidine [37], glucose[38] [39] and pH sensor [40]. Several groups have demonstrated E-DNA biosensors based on nw-PPy formed with template. The detection methods are based on the measure of resistance properties of polypyrrole layers using field effect transistors [41] or through the conductivity variation [42]. E-DNA based on amperometric measurements, with nw-PPy is still challenging, as the most demonstrated in literature are not conducting enough to allow high electron transfer and to provide amperometric measurement of attached redox marker.

In this work, we would like to prove that aligned nw-PPy, formed by electropolymerisation with template free, could be employed as transducer and provide chemical and electronic properties which improve the DNA immobilization and detection. We demonstrate that modification of nw-PPy could be achieved through electrochemical deposition of groups bearing amine such as ethylene diamine (EDA) and polyamidoamine dendrimers (PAMAM). Redox molecules such as ferrocene could be attached to PPy nanostructure to follow their electrical properties and their electron transfer ability. Such nanostructure could be applied for *M. tuberculosis* detection and discrimination of resistant stand with single nucleotide polymorphism. The results will be compared to other materials based on polypyrrole.

2. Material and methods

2.1 Reagents:

DNA sequences were obtained by Eurogentec Company. The DNA probes are with a sequence of 25 bases with a chain of six carbons and an amino group at its 5 ' phosphate position: NH_2- C6-5'TCA - ATC- GCT - GGA- TCA - ATC- ATG -TTA - G3'. The complementary DNA has a sequence of 25 bases: 5'CTA -ACA - TTG -AGA -TTC -GCC - AGA- TTG - A3 '. A non- complementary sequence of DNA also has been used: 5'CTA - ACA - TTG -AGA -TTC - TGA - CGA -GAT -GAT - CTT- C3 ' to study the selectivity of the biosensor. The DNA probe for *M. tuberculosis* is strand from rpob gene and is contained 18 bases with the sequences NH_2-C12-5'CCG-ACT-GTT-GGC-GCT-GGG3' and the DNA probe resistant drug with the mutation TTG in position 531 of *rpob* gene (TCG/TTG) NH_2-C12-5'CCG-ACT-GTC-GGC-GCT-GGG3'. The DNA of *M. Tuberculosis* is obtained by amplification of a fragment of 411 bp length of the *rpob* gene and the mutated one following the methods described previously [43].

Pyrrole, ethylene diamine (EDA), dendrimer polyamidoamine of second generation (PAMAM G2) and lithium perchlorate ($LiClO_4$), dibasic potassium phosphate (K_2HPO_4) were purchased from Sigma-Aldrich. The pyrrole is distilled before use. The (1,1'-(phtalimidebutanoate) ferrocene is bearing two acid activated by phtalimido groups and is obtained following the procedure described previously [44].

2.2 Biosensors formation

Electrodeposition of polypyrrole nanowire:

Films of nw-PPy were grown on the gold surface electrode by potentiostatic method during 2 minutes in a solution containing 0.15M pyrrole, 1 mM $LiClO_4$ and 0.2 M K_2HPO_4 in 5 mL of distilled water. During the electropolymerisation, the working and counter electrode were separated in a small volume cell from the reference electrode. After electrodeposition, the electrode was rinsed several times with double distilled water. Various applied potentials were studied 0.8V, 0.84 and 0.88 vs Ag/AgCl to underline their effect on polypyrrole morphology.

Functionalization of PPY with EDA and PAMAM G2 Dendrimers

The functionalization of nw-PPy by PAMAM was performed by CV in a solution of 1 µM of PAMAM and 0.5 M $LiClO_4$ by scanning the potential from 0 to 1.2 V at 50 mVs^{-1} during three cycles. This leads to a deposition of PAMAM on nw-PPy layer by covalent bonding and affords amine functions on the surface of PPy. The functionalization of nw-PPy with EDA was performed with the same method. The modified electrode with nw-PPy was placed in water solution containing 0.5 M $LiClO_4$ and 1M of EDA and the deposition was performed by scanning the potential from 0 to 0.7 V vs. Ag/AgCl during 10 cycles at scan rate of 50 mVs^{-1}. Then electrode was washed three times with double distilled water.

Covalent attachment of ferrocene and DNA Probe

These steps were carried out according the optimized procedures described in previous work [49]. Covalent attachment of ferrocene was performed by immersing the modified electrode nw-PPy-EDA or nw-PPy-PAMAM in a solution of acetonitrile containing 1µM ferrocene modified by two activated acid functions $Fc(NHP)_2$ during 1h at room temperature. The amide link was them formed between available amine groupes of the surface and ferrocene bearing two activated acid groups. The electrode was rinsed several times with acetonitrile and double distilled water to remove the non-attached ferrocene. The electrode was then immersed for one hour in a solution of PBS pH 7.4 containing 1µM of DNA probe modified by amino group in 5' end position. The reaction was performed at room temperature for one hour. The electrode was then rinsed with double-distilled water and PBS buffer.

Hybridization with DNA target

Hybridization between the DNA probe grafted on nw-PPy layer and the target DNA in solution was performed by incubating the biosensor into a target DNA solution for 30 min at 47° C. Hybridization was carried out with different concentrations of target DNA: 1 aM, 10 aM, 100 aM, 1fM, 10 fM, 100 fM. These concentrations were obtained by serial dilution of a stock solution. After incubation, the electrode was washed with PBS solution. Test of non-complementary targets was performed in the same condition to analyze the non-specific interactions on the biosensor.

2.3 Methods

The electrochemical measurements are based on a potensiostat biologic controlled with Eclab software. All electrochemistry measured was performed with a three-electrode cell with a

reference Ag/AgCl electrode, a platinum stem as counter electrode and a working electrode of gold with area of 0.03 cm^2. The working electrodes are polished several times with different thickness disc (6, 3, 1 µm) and diamond paste with respectively various thickness and subsequently activated in a sulfuric acid solution of 0.5 M by cyclic voltammetry by sweeping the potential between 0 to 1.8 V at 100 mV/S for 15 cycles.

X-ray photoelectron spectroscopy (XPS) was performed on a K Alpha spectrometer from Thermofisher, using monochromated X-ray source (Al Kα 1486, 6ev). The spectra obtained were treated by Advantage software provided by Thermo-Fisher. A Shirley-type background subtraction was used.

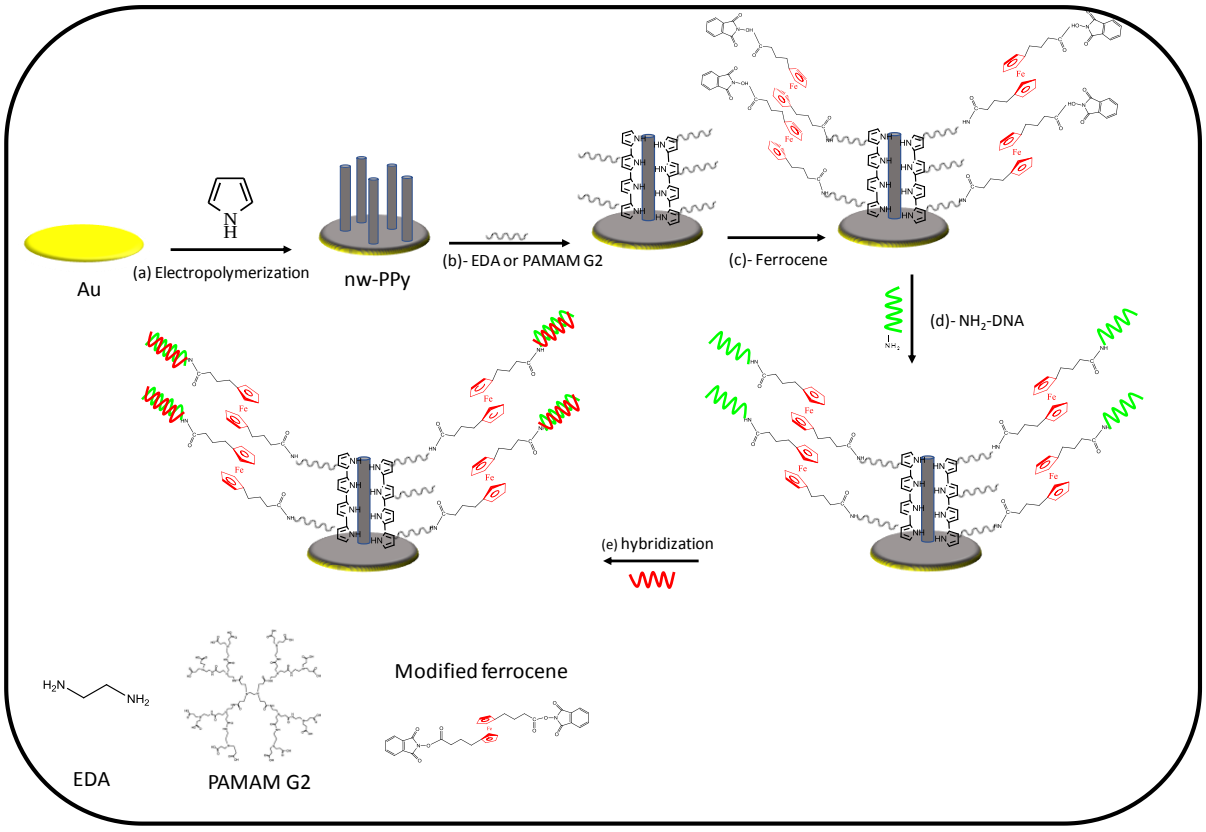

Figure 1: Schematic presentation of DNA biosensor based on modified nw-PPy: a) electro polymerization of nw-PPy film; b) electrodeposition of PAMAM G2; c) covalent grafting of ferrocene; d) anchoring of ssDNA probe; e) detection of specific DNA target

3. Results and discussions

3.1 Characterization of polypyrrole nanowires

SEM is used to analyze the surface morphology of the formed nw-PPy. The oriented nanowires structures are obtained following described methods using weak base of H_2PO_4 and low concentration of $LiCLO_4$. The polymers were obtained by potentiometric methods after optimization of potential applied and time of polymerization. The morphologies of nanowire such as long, shape, size and caliber could be controlled by the potential of polymerization. Figure 2 shows SEMs images of the electrode surface modified with nw-PPy formed using various potentials of electrodeposition. nw-PPy formed with applied potential of 0.88V underlines low organization of the nanowire and large width around 400 nm (Fig 2, image a). Decreasing the applied potential to 0.86V and 0.84V leads to lower width of nanowire and formation of array (Fig 2, images b et c). This proves the relationship between the potential applied for the polymerization and the structure of nanowire where applied potential has a large effect on the structure. The optimized condition retained thereafter is, applied potential of 0.84V during 120s. The wide of nanofibers are around 100 nm.

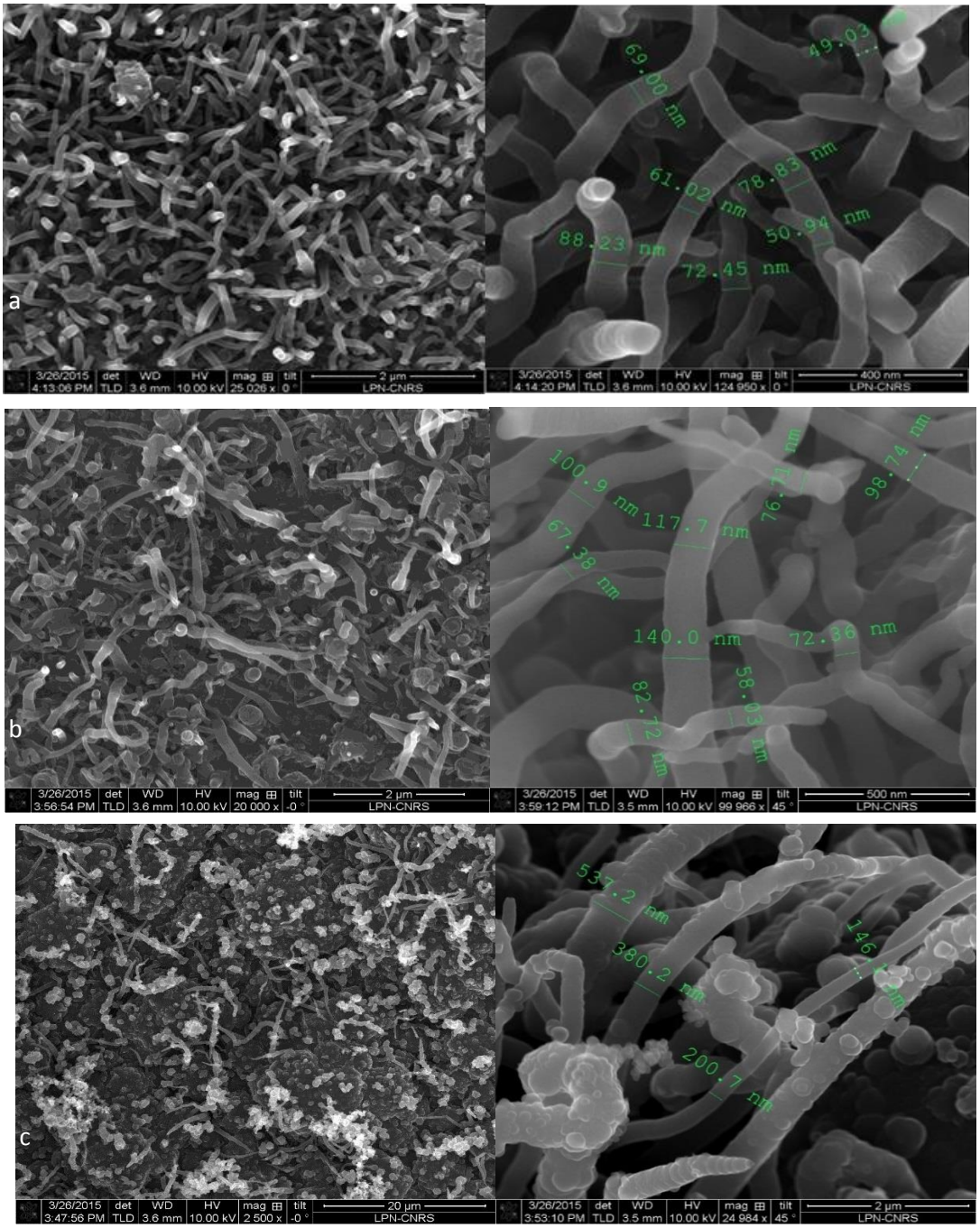

Figure 2: SEM images of gold surface covered by nw-PPy with different scale (20µm and 2µm) the films were formed with various applied potential a) E=0.84V; b) E=0.88V; c) E=0.80V.

The mechanism of the formation of nw-PPy film without using a template has challenged for a long time. The formation of nanowire has been explained by two hypotheses. The first

claims hydrogen interaction of amine of pyrrole and hydrogenophosphate ions $HPO_4^{2-}/H_2PO_4^-$ used as electrolyte is formed during nucleation process where the chemical environment favors hydrogen bonding. The oligomers of pyrrole formed during the first step is them self-align and form a well-ordered bundle structure on the surface where the grown of the PPy leads to aligned polypyrrole nanotubes on gold surface [31]. Another explanation was also provided, where the mechanism supposes the formation of self-assembled gas bubbles on the working electrode which could act as the chemical template for the growth of nw-PPy [45]. To confirm such mechanism, electropolymerisation of N-methyl pyrrole (Py-N-CH_3) has been performed in the same condition. SEM image shows that the polymerization process leads to the formation of nanowire (See SI.1, Figure S1). This demonstrates that the formation of nanowire polypyrrole could be obtained even for N-protected pyrrole and favors the mechanism of nanobubble of oxygen as template [32].

The electrical properties of the nw-PPy were analyzed through the electron transfer ability of redox process of $Fe(CN)_6^{4-}/Fe(CN)_6^{3-}$ system (Figure 3A). CVs show the response obtained with non-modified gold electrode and after the nw-PPy deposition. The CV shows high redox current obtained when gold coated nw-PPy. This demonstrates the formation of conducting polypyrrole layer with high surface area.

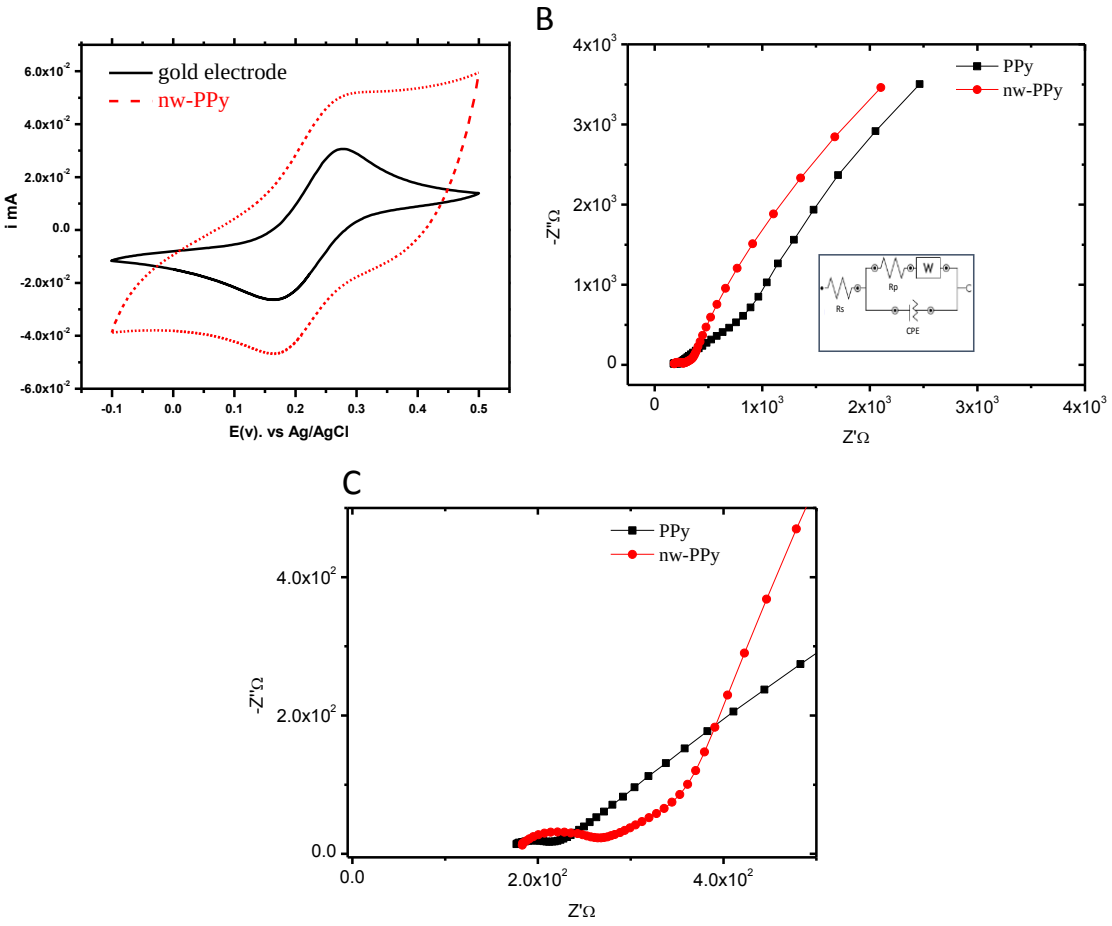

Figure 3: (A) Cyclic Voltammetry of the gold electrode analyzed in solution of $Fe(CN)_6^{4-}$ /$Fe(CN)_6^{3-}$ before and after polymerization with nw-PPy; (B) Nyquist plots obtained after modifications of gold electrode with PPy and nw-PPy the measurements were obtained in PBS buffer, in frequency range from 0.1Hz to 100 kHz at 0.10 V vs. Ag/AgCl by applying DC potential of 10 mV. The symbols are the experimental data, and the solid lines are the fitted curves using the equivalent circuit showed in inset. (C) Same Nyquist plot as (B) with enlargement in high frequency range.

Electrochemical impedance spectroscopy (EIS) measurement was realized with nw-PPy film and compact film of PPy in redox free PBS solution with applied potential of 0.1V near the open circuit potential to obtain low current flowing and avoid the lost of the stability at low frequency. This allows analyzing the electrical and electron transport properties of PPy layer. Nyquist plots (Figure 3B, C) were fitted according to the equivalent circuit model (inset Figure 3B, table S3), where one charge-transfer step is obtained according to bode and phase diagram. Various circuit models could be used to fit the PPy layer properties when EIS was

performed in the absence of redox markers. Some of them separate the ionic diffusion related to charge compensation and doping process from the electron transfer [46]. In this work where low potential range is applied, the circuit model with one interface fits well with the equivalent circuit presented. The measured charge transfer resistance could be related to the electrical properties of nw-PPy and its conductivity. Thus Rct informs on both the electron transfer occurred at the PPy as well as the anion transfer for charge compensation due to doping/undoping process. Result shown that nw-PPy has a characteristic of conducting surface where Rct value around 100 Ω which is in same order of magnitude of PPy compact film (See SI.3; table S3) and in the same order of magnitude of data described in literature [46]. The analytical treatment of EIS shows the presence of CPE behavior with n value of 0.8 instead of capacitance which demonstrates that the distribution of charge is not the same in all the thickness of the nanostructure. This behavior is generally observed in the case of nanostructured PPy [37].

3.2 Functionalization of nw-PPy and structural characterization

In order to functionalize nw-PPy with functional groups bearing amine in terminal position, electrochemical deposition of molecules containing amine groups were obtained through amine oxidation [47][48]. EDA could be attached to nw-PPy surface through formation of carbon-nitrogen link on the film layer, where the others terminal amine groups could serve for additional functionalization. To increase the number of functional groups dendrimers PAMAM of various generation could be attached with same way as demonstrated previously in the case of compacts film of PPy [49]. The surface of nw-PPy film was modified with EDA and dendrimers PAMAM of second generation (PAMAM G2). The modification was performed by scanning the potential and during oxidation, amine groups forms radical cations $–NH^{\bullet+}$ which interact with carbon of PPy leading to covalent grafting.

FT-IR and XPS were performed for the characterization of such reaction. FT-IR spectroscopy allowed analyzing the structural properties of nw-PPy before and after electrochemical deposition of amines. The spectra of nw-PPy and nw-PPy-PAMAM give significant information (See SI.2.1, Figure S2). The fundamental bands of nw-PPy related to the asymmetric (C=C) and symmetric (C=N) ring stretching vibration of pyrrole ring are observed at ~1545 and 1305 cm^{-1} respectively. The bands at 1175 and 903 cm^{-1} are characteristic of doped nw-PPy chains as demonstrated previously [50]. Covalent attachment

of dendrimers PAMAM leads to new bands at 1709 cm^{-1} attributed to the amide bond C=O of PAMAM.

XPS analysis, in carbon and nitrogen regions for nw-PPy and nw-PPy-PAMAM layers was also achieved (Fig. 4, table S1). The XPS spectrum in carbon region of nw-PPy showed five bands after deconvolution and peaks separations with maximum at 283.92, 284.82, 285.81, 287.65 and 290.94 (Fig. 4A). The two peaks at lowest energy correspond to α and β carbon atoms of nw-PPy. The peak (c) observed at 285.81 eV corresponds to imine C=N or $C\text{-}N^+$ structures and does at 287.65 eV could be associated to $C{=}N^+$ band. The peak (e) at 290.94 eV is much weaker and could be attributed to π-π* satellite commonly found in aromatic system. The spectrum obtained after PAMAM G2 electrodeposition (Fig. 4B) shows a significantly increase of the peaks ratio of 285.79 eV and 287.62 eV corresponding respectively to C-N and C=O bonds, which could be related to immobilized PAMAM G2.

In specific nitrogen region, nw-PPy layer was characterized with component of the peaks at 401 eV which could be attributed respectively to N-H bonds and to the positively charged nitrogen (Fig. 4C). Small contribution at 398.1 eV could be associated to aromatic amines structure. After modification of the surface with PAMAM G2, significant modifications of nw-PPy-PAMAM spectrum were observed (Fig. 4D). The nitrogen peaks showed two maximums at 399.80 and 401.36 eV which could be attributed to amine and amide bonds respectively. The relative intensity at 399.80 eV is much higher than for nw-PPy before modification and could correspond to C-N and N-H bonds of PAMAM G2 linked to the surface. The component at binding energy region of 401-403 eV corresponds usually to positively charged nitrogen, and the energy band obtained at 399.16 eV could be attributed to amines of PAMAM G2. These results confirm the association of PAMAM G2 dendrimers through covalent attachment to polymer.

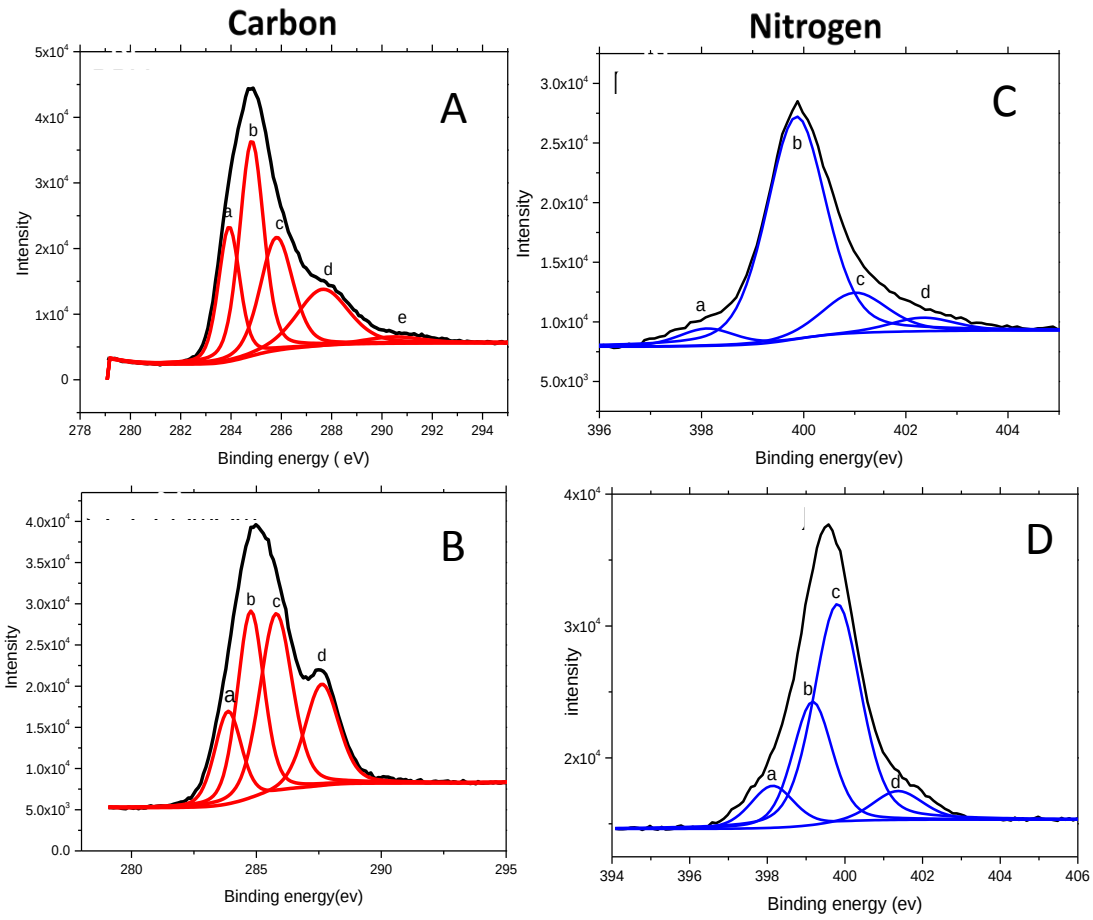

Figure 4: Deconvolution of XPS spectra in carbon and nitrogen for nw-PPy layer (A,C) and nw-PPy-PAMAM (B, D) after modification with PAMAM G2 dendrimers.

To demonstrate that the covalent attachment of PAMAM G2 to nw-PPy is through carbon-nitrogen link on pyrrole ring and not nitrogen-nitrogen between the amine of polypyrrole and PAMAM, electrodeposition of PAMAM was realized also on nw-PPy-N-CH_3 modified in nitrogen by methyl group. XPS analysis was then used for further investigation on PPy-N-CH_3 and PPy-N-CH_3-PAMAM (see SI.2.2, Figure S3, Table S2). The deconvolution of N_{1S} in the case of PPy-N-CH_3 gives one peak 399,9 eV related to carbon-nitrogen bond. After grafted of PAMAM in PPy-N-CH_3 the nitrogen region shows after deconvolution a peak related to carbon-nitrogen bond and new peak at 402.4 which could be attributed to nitrogen positively charged in PAMAM. This result proves that the PAMAM groups are well grafted on the surface of PPy-N-CH_3 and this link is between the nitrogen of PAMAM and carbon β of pyrrole.

3.3 Electrochemical characterization of modified nw-PPy

Electrochemical characterization through EIS measurements allowed the characterization of electrical properties of the nw-PPy modified with PAMAM and EDA and the comparison with non-structured PPy (Figure 5). Nyquist plots were performed in PBS solution free of redox markers. The EIS data were successfully fitted by the same equivalent circuit model as shown previously (Figure 3B inset). For the two PPy and nw-PPy, an important increase in the resistance was observed after PAMAM immobilization (Figure 5 A, B and Table S3). The enlargement in high frequency region demonstrates well the small semicircle obtained in the case of the non-modified PPy and nw-PPy compared to those obtained after modification (See SI.3, Figure S4). This is due to the saturation of the surface with larges molecules such as PAMAM which has generally positive charge causing blocking effect. This behavior is more important in the case of nw-PPy-PAMAM than PPy-PAMAM (Figure 5C). This could be attributed to larger amount of the dendrimers covalently bonded to nw-PPy which present higher surface to volume ratio compared to PPy. In the case of surface nw-PPy-EDA (Figure 5D) smaller variation of the charge transfer resistance is obtained due the small size of EDA molecules.

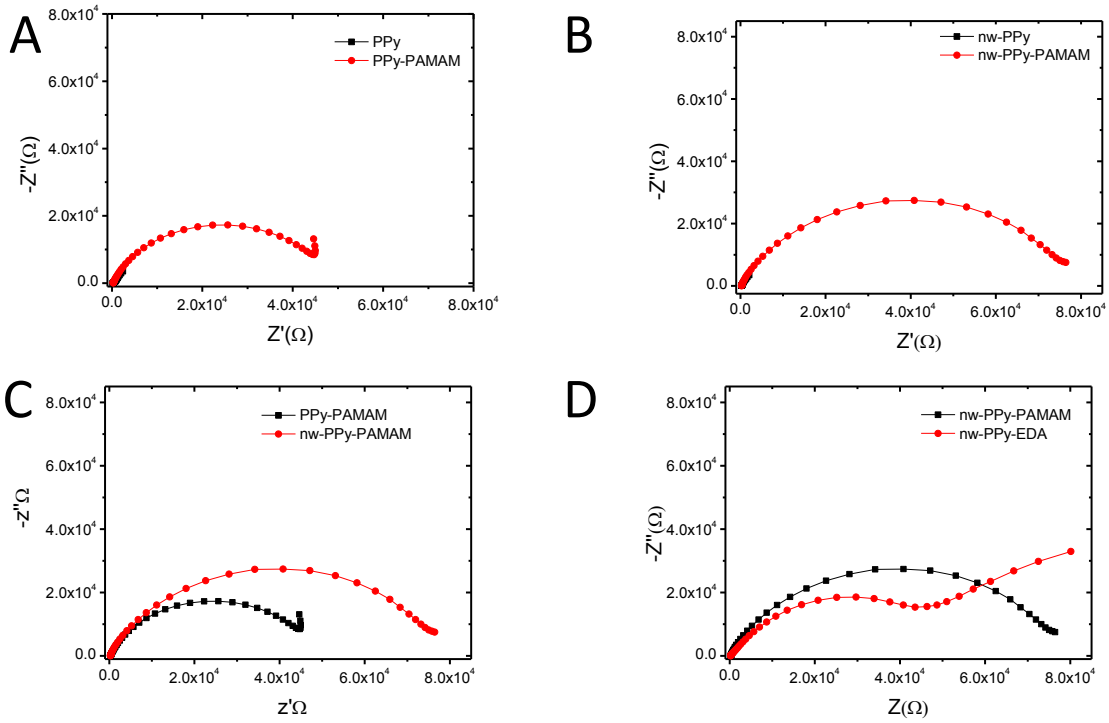

Figure 5: Nyquist plots obtained after attachment of dendrimers PAMAM G2 on PPy(A) and nw-PPy(B) and (C) comparison of response obtained between structured and non structured

surface; (D) comparison of ESI obtained after the attachment of EDA or PAMAM to nw-PPy. The measurements were obtained in PBS buffer, in frequency range from 0.1Hz to 100 kHz at 0.10 V vs. Ag/AgCl by applying DC potential of 10 mV. (C) Comparison between PPy-PAMAM-FC and nw-PPy-PAMAM-FC. The symbols are the experimental data, and the solid lines are the fitted curves using the equivalent circuit showed in Figure 3.

Association of ferrocene redox marker to the nw-PPy-PAMAM and nw-PPy-EDA was realized to enhance the kinetic of charge transfer within the nw-PPy layer and to study the electron transfer ability. Ferrocene bearing two activated acid groups (N-Hydroxyphtalimide) could react on both the surface of the aminated surface of PPy and the DNA probe bearing amine group in terminal 5'position. After the attachment of ferrocene, the nw-PPy/EDA/Fc and nw-PPy/PAMAMG2/Fc films were analyzed by CV and square wave voltammetry (SWV) (Figure 6). Redox signal of ferrocene with oxidation peak at 0.09 V (vs. Ag/AgCl) and reduction peak at 0.04 V (vs. Ag/AgCl) are obtained after ferrocene attachment on modified nw-PPy-PAMAM and nw-PPy-EDA. The variation of anodic and cathodic peak potential gives a value of 50mV which demonstrated non-ideality reversible redox system. The formal potential measured is 0.05 V vs Ag/AgCl which is lower compared to ferrocene attached to others surface and nanomaterials (see Table 1). The shift toward lower potentials of ferrocene compared to others materials may be explained by the polar properties of nw-PPy which is known as super hydrophilic structures [51]. SWVs (Figure 6 B) show well-defined peaks of oxidation of ferrocene where the current is much higher for the nw-PPy-PAMAM than that modified with EDA. This result demonstrates clearly that nw-PPy-PAMAM allows to bind a large numbers of redox markers compared to nw-PPy-EDA. The full-widths at half-maximum (fwhm) of the oxidation peaks could give information about the homogeneity and the distribution of redox molecules on the surface. The theoretical value of fwhm of redox reversible redox center immobilized on the surface is expected at 91mV at 25°C [52]. Analysis of electrochemical characteristic of ferrocene attached to nw-PPy through EDA or PAMAM demonstrate that fwhm is 146 mV in both case which is higher that the ideally a one-electron transfer and also higher of monolayer of ferrocene calculated at 114mV[53]. The increased value of fwhm could be related to chemical inhomogeneity of the surface or the interaction between neighboring ferrocene. In the last case, dilutions of redox site by spacing their attachment leads to decrease fwhm. Concerning nw-PPy the same value is obtained with

both nw-PPy modified with EDA and PAMAM G2. This underlines that the higher value of fwhm is related to the inhomogeneity of the surface of nw-PPy. Similar report has been demonstrated in the case of ferrocene anchored on nanofiber of carbon where large value has been attributed to the presence of different local environments of the redox couple [54] [55].

The charge exchanged during redox process allows calculation of the surface coverage of ferrocene groups, bonded to the modified nw-PPy, following the equation:

$$\Gamma = Q / nFA \qquad (1)$$

Γ is surface coverage, Q is the charge under the cathodic or anodic waves, n is number of electrons involved in the redox process, F is the Faraday constant, and A is the area of the electrode.

Based on equation (1) we calculated the average coverage of the surface for nw-PPy nanowires modified with EDA and with PAMAM G2 (see table 1). Immobilization of ferrocene on nw-PPy-EDA leads to surface coverage of 49.10^{-9} mole.cm^{-2}, where surface coverage of 64.10^{-9} mole.cm^{-2} is obtained in the case of nw-PPy-PAMAM. This confirms that the formation of the nano-array of polypyrrole improves the surface area and then the number of attached molecules.

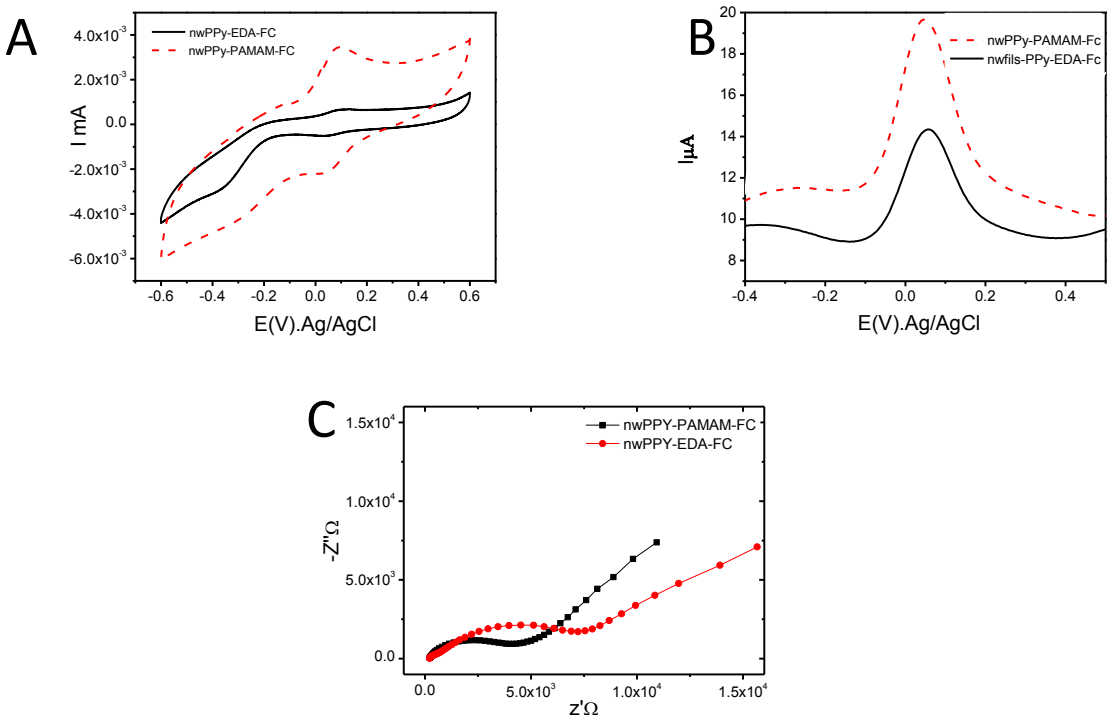

Figure 6: (A) CV (B) SWV of electrochemical signal of ferrocenyl group (Fc) linked to nw-PPy modified with dendrimers PAMAM and EDA, (C) Nyquist plots obtained after covalent attachment of ferrocene to the nw-PPy-PAMAM and nw-PPy-EDA modified electrode. The measurements were obtained in PBS buffer, in frequency range from 0.1Hz to 100 kHz at 0.10 V vs. Ag/AgCl by applying DC potential of 10 mV. The symbols are the experimental data, and the solid are the fitted curves using the equivalent circuit.

EIS were performed after covalent attachment of electroactive ferrocene for both modified electrodes nw-PPy-PAMAM-Fc and nw-PPy-EDA-Fc. Nyquist plots show a decrease in semi-circle after ferrocene attachment which underlines lower charge transfer resistance (Fig. 6C, Table S3). This proves that the bonding of the electroactive species to the modified electrode surface increase the charge transfer ability. ESI shows a more significant decrease of charge transfer resistance in case of nw-PPy-PAMAM-Fc compared nw-PPy-EDA-Fc. This confirm the previously result demonstrating that the number of ferrocene grafted on the surface of modified electrode is higher in the case of PAMAM immobilization increasing the charge transfer ability.

3.4 Kinetic characterizations of attached ferrocene on nw-PPy

To understand how the structure of polypyrrole, impact the electron transfer process, the electron-transfer rate constants are calculated from the peak-to-peak separation of CVs using Laviron method [52]. The method uses the numerical integration to correlate the standard electron-transfer rate constant ks with the separation between anodic peaks ΔEp at different scan rates (equation 2).

$$\frac{1}{m} = \frac{nvF}{RT}\frac{1}{K_S} \qquad (2)$$

Where n is number of electrons exchanged in the redox reaction (n=1), v is the scan rate m is the dimensionless rate constant, R is universal gas constant, T temperature, F faraday constant. The value of m was determined by adjustment of the curve $\Delta Ep = f(m^{-1})$.

The k_s calculated for ferrocene attached on nw-PPy-PAMAM-Fc was measured and compared to PPy-PAMAM-Fc layer obtained by binding of PAMAM to compact PPy film [49]. An increase of k_s from (1.67±0.01) s^{-1} to (7.44±0.03) s^{-1} was obtained in the case of nw-PPy-PAMAM-Fc compared to compact layer. This demonstrates that the nanowires improve the electron transfer between neighboring ferrocene. This improvement of the ks could be related to the large surface area of nanowire PPy and their chemical properties which favor the electron hopping process. To test how the molecular length affects the electron-transfer process, the CV data obtained with nw-PPy-EDA-Fc with attached EDA, smaller molecule compared to PAMAM, were analyzed. The data showed that there are significant change in the electron transfer rate constant as the length of the carbon chain is varied from PAMAM to EDA with increase of the k_s from (7.44±0.03) to (18.77±0.06) respectively.

	Eox (V)	Γ(mole.cm^{-2})	Ks (s^{-1})	LOD	Ref
Nanowire PPY-EDA-Fc	0.054	49.10^{-9} ±1.15	18,7	-	This work

Nanowire PPY-PAMAM-Fc	0.05	$64 .10^{-9} \pm 1.02$	7.4	0.36aM	This work
PPY-PAMAM-Fc	0.135	$18.87.10^{-9} \pm 1.14$	1.6	0.4fM	[56]
PPY-CONH-PAMAM-Fc	0.11	$3.0.10^{-9} \pm 0.04$	5.8	-	[57]
PPY-CNT-PAMAM-Fc	0.256	$32\ 10^{-9} \pm 2$	1.90	0.3fM	[43]

Table 1: Electrochemical parameters obtained for various modified polypyrrole structures

3.5 Properties of biosensors towards DNA detection

To study the effects of nanostructured polypyrrole in sensing properties, the covalent attachment of DNA and then hybridization reaction between ssDNA probe immobilized and DNA target in solution has been realized. The concentration range of DNA target studied was from 1aM to 1 pM. This was measured by the changes of current corresponding to redox signal of ferrocene attached to the nw-PPy. SWVs show the variation of the redox current after DNA hybridization within the various concentrations (Figure 7A). The decrease of redox current is related to the low electron transfer happened after the hybridization of complementary DNA and the formation of double strand on the surface. This current variation is depending on the concentration of DNA target in solution. Calibration curve was plotted by presenting the average current variation versus the logarithmic scale of the concentration (Figure 7B). We can see that large dynamic range of DNA detection is obtained with this biosensor from 1 aM to 100fM where the saturation is started at 100fM. The calculated detection limit of 0.36 aM is obtained, based on signal-to-noise ratio of 3 and by measuring the standard deviation of the blank test. This sensitivity could be related to various parameters provided by polypyrrole nanostructure and their functionalization such as the high surface area of nw-PPy, that allows loading a large amount of DNA probe, the conductivity of the nw-PPy layer and hydrophilic character, which enhances the electron transfer ability. This result demonstrates the potential of nanowire polypyrrole formed by electrodeposition as platform for DNA detection.

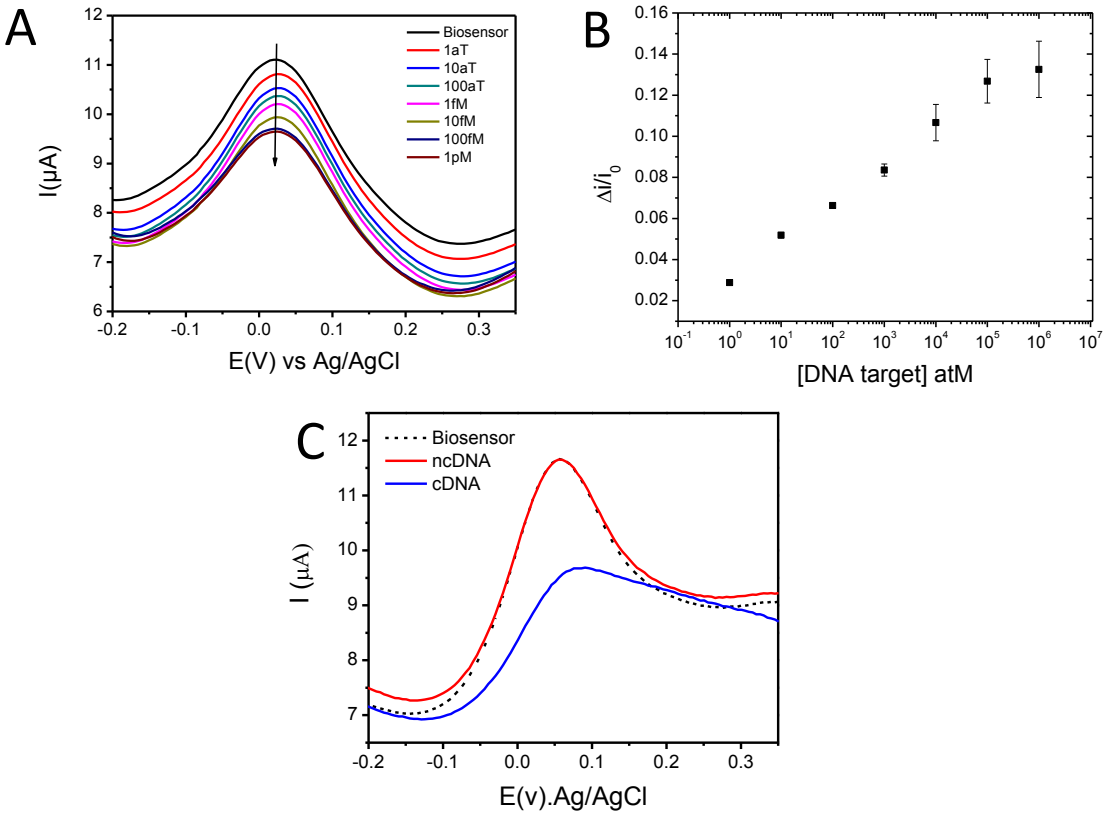

Figure 7: (A) SWV recorded in PBS solution after incubation of biosensor with various DNA concentrations (1aM–100 fM). (B) Plot of the relative changes of the current peak vs. concentration of DNA target $\Delta I=(I_0-I)/I_0$, where I_0 is the peak current of biosensor and I the current measured after incubation of the biosensor with certain concentration of DNA target. (C) SWV obtained after incubation of biosensors the 1µM of ncDNA and 1fM of c DNA target.

3.6 Analysis of the performance of the E-DNA biosensors

The non-specific interactions were studied by incubation the biosensor with non-complementary DNA target of 18 bases. Figure 7C shows the SWV analysis before incubation of electrode in DNA solutions and after incubation in 1 µM solution of DNA non-complementary target (nc DNA) and 1 fM of DNA target (c DNA). No decrease of the redox current after hybridization with nc DNA target was observed, while the incubation with cDNA in the lower concentration of 1fM showed a large variation. This underlines that the chemical structure of nw-PPy prevents non-specific interaction. This could be related to

super-hydrophilic character of nw-PPy as their polar and hydrated environment surface which disfavors the interaction of the relatively hydrophobic nucleobase of DNA [58].

The reproducibility was tested by measuring the response with 3 fresh biosensors and standard deviation of 10% is measured. This reproducibility could be improved by controlling the surface properties of the gold and the geometry of the cell.

3.7. Detection in real sample of *M. Tuberculosis* and resistant strand

The biosensor was used also for detection of DNA pathogen agent of *M. tuberculosis*, and was applied to discriminate the single nucleotide polymorphism (SNP) (TCG/TTG) which gives the resistance of *M.tuberculosis* to rifampicin drug. The PCR sample were composed of 411 bases of DNA fragment from rpoB gene called WT, and fragment with mutated DNA called Mut. The DNA probe specific to WT and Mut was composed of 18 bases modified with amine group and was attached to the nw-PPY surface. The hybridization reaction with WT and Mut DNA was followed by SWV of redox signal of ferrocene (Figure 8).

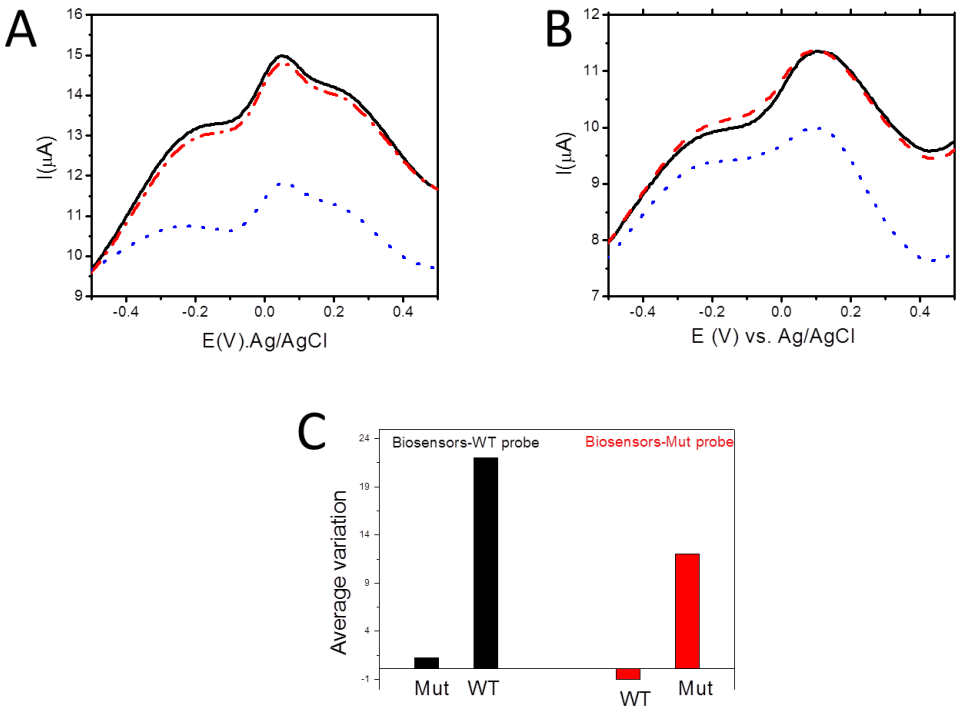

Figure 8: (A) SWV response obtained with biosensors modified with WT probe (solid line) and after detection with PCR sample with mutated DNA (dash line) and after detection with PCR sample with

WT DNA (dot line). (B) SWV response of biosensors obtained with biosensors modified with Mut probe (solid line) and after detection with PCR sample with WT DNA (dash line) and after detection with PCR sample with Mut DNA(dot line). (C) Histogram resuming average variation of current with the various biosensors with WT and Mut DNA probe and target from PCR sample.

The incubation the biosensor bearing WT probe with the PCR sample with the SNP Mut sample with mutation shows small variation in the response of biosensor (Figure 8A, red curve). However, when the biosensors hybridize specific WT DNA target large variation is obtained (Figure 8A, green curve). The same results were obtained when biosensor bearing DNA probe with the mutated TCG/*TTG*. Large variation is obtained with mutated DNA sample and very small variation in the case of WT sample (Figure 8B). These results demonstrate that biosensors based on nw-PPy was able to analyze DNA from real sample of *M. tuberculosis* strains and to distinct the SNP mutation which is a very promising in their application in DNA sensors.

This biosensors present high sensitivity and easy to used compared to those demonstrated in the case of DNA biosensors were amplification steps is generally needed after the DNA hybridization step (see table 2).

Table 2: Comparison of the present method for *M. tuberculosis* detection with other reported works based on electrochemical biosensors. (AuNPs Gold nanoparticles; RGO reduced graphene oxide; MPs magnetic nanoparticles, PANi polyaniline; ALP Alkaline phosphatase, MB methylene blue)

Biosensor	Method of detection or amplification	Detection limit	Dynamic range	References
Dextrin/AuNPs	Amplification MPs/AuNPs	0.01ng/µl	0.01-10 ng/µl	[59]
CNT/ZrO_2	impedimetric	0.065 ng/µl	1-150ng/µl	[60]

RGO/AuNP	AuNPs/PANI assisted signal amplification	1fM	1fM-1nM	[61]
ITO/AuNPs	Dual amplification AuNPs and ALP	1.25ng/ml	1.25-50ng/ml	[62]
polypyrrole–polyvinylsulphonate /	Redox signal of MB intercalator	0.1ng/µl	0.1-1.2ng/µl	[63]
PPy/Fe_3O_4	Redox signal	1fM	1fM-0.1pM	[64]
Nw-PPy-	Amperometric	0.36aM	0.1aM to 100fM	Present work

4. Conclusion

Nanowire polypyrrole formed by template free with simple electropolymerization could be used as sensitive E-DNA biosensors through amperometric measurement. We demonstrated that nw-PPy could be formed by template free and highlight the mechanism of their formation as well as high electrical properties. The obtained nw-PPy could be modified through EDA or PAMAM electrodeposition through carbon-nitrogen coupling reaction which leads to introduction of aminated surface. Covalent attachment of ferrocene as redox marker on the modified nw-PPy could be performed and the electrochemical properties exhibits lower redox potential and high rate of electron transfer ($18s^{-1}$). This is obtained thanks to high hydrophilic chemical structure character, good conductivity and high surface area of nw-PPy. E-DNA biosensor based on nw-PPy modified with ferrocene as redox marker shows a detection limit of 0.36aM without any amplification procedure. Improvement of the sensitivity to DNA hybridization was demonstrated compared to compact PPy layer and others nanostructured materials. Their selectivity was proven by their ability to discriminate rpob gene of *M.Tuberculosis* from mutated with single polymorphism. The biosensors are able to measure DNA from complex sample such as PCR. These analytical performances properties were

obtained by dint of the chemical and electronic properties and their soft functionalization through amine oxidation. Thus, high surface area of nw-PPy allows loading a large amount of DNA probe, the conductivity of the nw-PPy layer enhances electron transfer ability, where hydrophilic character of nw-PPy prevents non-specific interaction. The developed electrochemical DNA based on nw-PPy could be used as platform for detection of various biomolecules in complex sample involving specific bioreceptor.

Acknowledgments:

The authors' acknowledge University Paris-Saclay and CNRS for finding this project and thanks the Lebanese government for the PhD fellowship. The project PHC N° 39382RE is acknowledged for supporting a part of this project.

References

[1] V. Gubala, L.F. Harris, A.J. Ricco, M.X. Tan, D.E. Williams, Point of Care Diagnostics: Status and Future, Anal. Chem. 84 (2012) 487–515. doi:10.1021/ac2030199.
[2] J. C. Jokerst, J. M. Emory, C. S. Henry, Advances in microfluidics for environmental analysis, Analyst. 137 (2012) 24–34. doi:10.1039/C1AN15368D.
[3] Y.T. Atalay, S. Vermeir, D. Witters, N. Vergauwe, B. Verbruggen, P. Verboven, B.M. Nicolaï, J. Lammertyn, Microfluidic analytical systems for food analysis, Trends Food Sci. Technol. 22 (2011) 386–404. doi:10.1016/j.tifs.2011.05.001.
[4] C. Mengoli, M. Cruciani, R.A. Barnes, J. Loeffler, J.P. Donnelly, Use of PCR for diagnosis of invasive aspergillosis: systematic review and meta-analysis, Lancet Infect. Dis. 9 (2009) 89–96. doi:10.1016/S1473-3099(09)70019-2.
[5] S.A. Bustin, R. Mueller, Real-time reverse transcription PCR (qRT-PCR) and its potential use in clinical diagnosis, Clin. Sci. 109 (2005) 365–379. doi:10.1042/CS20050086.
[6] H.-B. Wang, Y. Li, H.-Y. Bai, Y.-M. Liu, DNA-templated Au nanoclusters and MnO2 sheets: a label-free and universal fluorescence biosensing platform, Sens. Actuators B Chem. 259 (2018) 204–210. doi:10.1016/j.snb.2017.12.048.
[7] H.-B. Wang, H.-Y. Bai, G.-L. Dong, Y.-M. Liu, DNA-templated Au nanoclusters coupled with proximity-dependent hybridization and guanine-rich DNA induced quenching: a sensitive fluorescent biosensing platform for DNA detection, Nanoscale Adv. 1 (2019) 1482–1488. doi:10.1039/C8NA00278A.
[8] D.C. Ferrier, M.P. Shaver, P.J.W. Hands, Micro- and nano-structure based oligonucleotide sensors, Biosens. Bioelectron. 68 (2015) 798–810. doi:10.1016/j.bios.2015.01.031.
[9] K.J. Odenthal, J.J. Gooding, An introduction to electrochemical DNAbiosensors, Analyst. 132 (2007) 603–610. doi:10.1039/B701816A.
[10] H. Peng, L. Zhang, C. Soeller, J. Travas-Sejdic, Conducting polymers for electrochemical DNA sensing, Biomaterials. 30 (2009) 2132–2148. doi:10.1016/j.biomaterials.2008.12.065.
[11] S. Cosnier, M. Holzinger, Biosensors based on electropolymerized films., in: Electropolymerization, Wiley-VCH Verlag GmbH & Co. KGaA, 2010: pp. 189–213. doi:10.1002/9783527630592.ch10.
[12] D.D. Ateh, H.A. Navsaria, P. Vadgama, Polypyrrole-based conducting polymers and interactions with biological tissues, J. R. Soc. Interface. 3 (2006) 741–752. doi:10.1098/rsif.2006.0141.

[13] H. Korri-Youssoufi, A. Yassar, Electrochemical Probing of DNA Based on Oligonucleotide-Functionalized Polypyrrole, Biomacromolecules. 2 (2001) 58–64. doi:10.1021/bm0000440.
[14] H.Q.A. Lê, S. Chebil, B. Makrouf, H. Sauriat-Dorizon, B. Mandrand, H. Korri-Youssoufi, Effect of the size of electrode on electrochemical properties of ferrocene-functionalized polypyrrole towards DNA sensing, Talanta. 81 (2010) 1250–1257. doi:10.1016/j.talanta.2010.02.017.
[15] H. Korri-Youssoufi, P. Godillot, P. Srivastava, A. El Kassmi, F. Garnier, New method of polypyrrole functionalization toward molecular recognition, Synth. Met. 84 (1997) 169–170. doi:10.1016/S0379-6779(97)80697-2.
[16] C. Tlili, H. Korri-Youssoufi, L. Ponsonnet, C. Martelet, N.J. Jaffrezic-Renault, Electrochemical impedance probing of DNA hybridisation on oligonucleotide-functionalised polypyrrole, Talanta. 68 (2005) 131–137. doi:10.1016/j.talanta.2005.04.069.
[17] A. Ramanaviciene, A. Ramanavicius, Pulsed amperometric detection of DNA with an ssDNA/polypyrrole-modified electrode., Anal. Bioanal. Chem. 379 (2004) 287–293. doi:10.1007/s00216-004-2573-6.
[18] H. Korri-Youssoufi, B. Makrouf, Electrochemical biosensing of DNA hybridization by ferrocenyl groups functionalized polypyrrole, Anal. Chim. Acta. 469 (2002) 85–92. doi:10.1016/S0003-2670(02)00539-1.
[19] V. Ratautaite, S.N. Topkaya, L. Mikoliunaite, M. Ozsoz, Y. Oztekin, A. Ramanaviciene, A. Ramanavicius, Molecularly Imprinted Polypyrrole for DNA Determination, Electroanalysis. 25 (2013) 1169–1177. doi:10.1002/elan.201300063.
[20] A. Khodadadi, E. Faghih-Mirzaei, H. Karimi-Maleh, A. Abbaspourrad, S. Agarwal, V.K. Gupta, A new epirubicin biosensor based on amplifying DNA interactions with polypyrrole and nitrogen-doped reduced graphene: Experimental and docking theoretical investigations, Sens. Actuators B Chem. 284 (2019) 568–574. doi:10.1016/j.snb.2018.12.164.
[21] S. Cheraghi, M.A. Taher, H. Karimi-Maleh, E. Faghih-Mirzaei, A nanostructure label-free DNA biosensor for ciprofloxacin analysis as a chemotherapeutic agent: an experimental and theoretical investigation, New J. Chem. 41 (2017) 4985–4989. doi:10.1039/C7NJ00609H.
[22] Rajesh, T. Ahuja, D. Kumar, Recent progress in the development of nano-structured conducting polymers/nanocomposites for sensor applications, Sens. Actuators B Chem. 136 (2009) 275–286. doi:10.1016/j.snb.2008.09.014.
[23] C. Debiemme-Chouvy, A. Fakhry, F. Pillier, Electrosynthesis of polypyrrole nano/micro structures using an electrogenerated oriented polypyrrole nanowire array as framework, Electrochimica Acta. 268 (2018) 66–72. doi:10.1016/j.electacta.2018.02.092.
[24] A. Nazemi, A. Najafian, S.A. Seyed Sadjadi, Aluminium oxide nanowires synthesis from high purity aluminium films via two-step anodization, Superlattices Microstruct. 81 (2015) 1–6. doi:10.1016/j.spmi.2015.01.013.
[25] I. Sameera, R. Bhatia, V. Prasad, R. Menon, Temperature dependent current-voltage characteristics of zinc oxide nanowire/polypyrrole nanocomposite, Appl. Phys. Lett. 105 (2014) 232112. doi:10.1063/1.4903923.
[26] T.L. Tran, T.X. Chu, P.Q. Do, D.T. Pham, V.V.Q. Trieu, D.C. Huynh, A.T. Mai, In-channel-grown Polypyrrole Nanowire for the Detection of DNA Hybridization in an Electrochemical Microfluidic Biosensor, J Nanomater. 2015 (2015) 2:2–2:2. doi:10.1155/2015/458629.
[27] A. Errachid, D. Caballero, E. Crespo, F. Bessueille, M. Pla-Roca, C.A. Mills, F. Teixidor, J. Samitier, Electropolymerization of nano-dimensioned polypyrrole micro-ring arrays on gold substrates prepared using submerged micro-contact printing, Nanotechnology. 18 (2007) 485301. doi:10.1088/0957-4484/18/48/485301.
[28] X. Zhang, S.K. Manohar, Bulk Synthesis of Polypyrrole Nanofibers by a Seeding Approach, J. Am. Chem. Soc. 126 (2004) 12714–12715. doi:10.1021/ja046359v.
[29] D. Plausinaitis, L. Sinkevicius, L. Mikoliunaite, V. Plausinaitiene, A. Ramanaviciene, A. Ramanavicius, Electrochemical polypyrrole formation from pyrrole ‘adlayer,’ Phys. Chem. Chem. Phys. 19 (2017) 1029–1038. doi:10.1039/C6CP06545G.

[30] D. Plausinaitis, V. Ratautaite, L. Mikoliunaite, L. Sinkevicius, A. Ramanaviciene, A. Ramanavicius, Quartz Crystal Microbalance-Based Evaluation of the Electrochemical Formation of an Aggregated Polypyrrole Particle-Based Layer, Langmuir. 31 (2015) 3186–3193. doi:10.1021/la504340u.
[31] L. Qu, G. Shi, J. Yuan, G. Han, F. Chen, Preparation of polypyrrole microstructures by direct electrochemical oxidation of pyrrole in an aqueous solution of camphorsulfonic acid, J. Electroanal. Chem. 561 (2004) 149–156. doi:10.1016/j.jelechem.2003.07.028.
[32] C. Debiemme-Chouvy, Template-free one-step electrochemical formation of polypyrrole nanowire array, Electrochem. Commun. 11 (2009) 298–301. doi:10.1016/j.elecom.2008.11.030.
[33] S. Aravamudhan, S. Bhansali, Development of micro-fluidic nitrate-selective sensor based on doped-polypyrrole nanowires, Sens. Actuators B Chem. 132 (2008) 623–630. doi:10.1016/j.snb.2008.01.046.
[34] M. Lin, M. Cho, W.-S. Choe, J.-B. Yoo, Y. Lee, Polypyrrole nanowire modified with Gly-Gly-His tripeptide for electrochemical detection of copper ion, Biosens. Bioelectron. 26 (2010) 940–945. doi:10.1016/j.bios.2010.06.030.
[35] L. Zhang, F. Meng, Y. Chen, J. Liu, Y. Sun, T. Luo, M. Li, J. Liu, A novel ammonia sensor based on high density, small diameter polypyrrole nanowire arrays, Sens. Actuators B Chem. 142 (2009) 204–209. doi:10.1016/j.snb.2009.07.042.
[36] H.-H. Yang, S.-Q. Zhang, F. Tan, Z.-X. Zhuang, X.-R. Wang, Surface Molecularly Imprinted Nanowires for Biorecognition, J. Am. Chem. Soc. 127 (2005) 1378–1379. doi:10.1021/ja0467622.
[37] K. Ghanbari, S.Z. Bathaie, M.F. Mousavi, Electrochemically fabricated polypyrrole nanofiber-modified electrode as a new electrochemical DNA biosensor, Biosens. Bioelectron. 23 (2008) 1825–1831. doi:10.1016/j.bios.2008.02.029.
[38] L. Liu, N. Jia, Q. Zhou, M. Yan, Z. Jiang, Electrochemically fabricated nanoelectrode ensembles for glucose biosensors, Mater. Sci. Eng. C. 27 (2007) 57–60. doi:10.1016/j.msec.2006.02.002.
[39] H. Jiang, A. Zhang, Y. Sun, X. Ru, D. Ge, W. Shi, Poly(1-(2-carboxyethyl)pyrrole)/polypyrrole composite nanowires for glucose biosensor, Electrochimica Acta. 70 (2012) 278–285. doi:10.1016/j.electacta.2012.03.064.
[40] G.D. Sulka, K. Hnida, A. Brzózka, pH sensors based on polypyrrole nanowire arrays, Electrochimica Acta. 104 (2013) 536–541. doi:10.1016/j.electacta.2012.12.064.
[41] M.A. Bangar, D.J. Shirale, H.J. Purohit, W. Chen, N.V. Myung, A. Mulchandani, Single Conducting Polymer Nanowire Based Sequence-Specific, Base-Pair-Length Dependant Label-free DNA Sensor, Electroanalysis. 23 (2011) 371–379. doi:10.1002/elan.201000388.
[42] A.T. Mai, T.P. Duc, X.C. Thi, M.H. Nguyen, H.H. Nguyen, Highly sensitive DNA sensor based on polypyrrole nanowire, Appl. Surf. Sci. 309 (2014) 285–289. doi:10.1016/j.apsusc.2014.05.032.
[43] A. Miodek, N. Mejri, M. Gomgnimbou, C. Sola, H. Korri-Youssoufi, E-DNA Sensor of Mycobacterium tuberculosis Based on Electrochemical Assembly of Nanomaterials (MWCNTs/PPy/PAMAM), Anal. Chem. 87 (2015) 9257–9264. doi:10.1021/acs.analchem.5b01761.
[44] P. Godillot, H. Korri-Youssoufi, P. Srivastava, A. El Kassmi, F. Garnier, Direct chemical functionalization of as-grown electroactive polypyrrole film containing leaving groups, Synth. Met. 83 (1996) 117–123. doi:10.1016/S0379-6779(97)80064-1.
[45] A. Fakhry, H. Cachet, C. Debiemme-Chouvy, Mechanism of formation of templateless electrogenerated polypyrrole nanostructures, Electrochimica Acta. 179 (2015) 297–303. doi:10.1016/j.electacta.2015.03.025.
[46] A. Ramanavicius, A. Finkelsteinas, H. Cesiulis, A. Ramanaviciene, Electrochemical impedance spectroscopy of polypyrrole based electrochemical immunosensor, Bioelectrochemistry. 79 (2010) 11–16. doi:10.1016/j.bioelechem.2009.09.013.
[47] M. A. Ghanem, J.-M. Chrétien, A. Pinczewska, J. D. Kilburn, P. N. Bartlett, Covalent modification of glassy carbon surface with organic redox probes through diamine linkers using

electrochemical and solid-phase synthesis methodologies, J. Mater. Chem. 18 (2008) 4917–4927. doi:10.1039/B809040H.
[48] J.-M. Chrétien, M.A. Ghanem, P.N. Bartlett, J.D. Kilburn, Covalent Tethering of Organic Functionality to the Surface of Glassy Carbon Electrodes by Using Electrochemical and Solid-Phase Synthesis Methodologies, Chem. – Eur. J. 14 (2008) 2548–2556. doi:10.1002/chem.200701559.
[49] A. Miodek, N. Mejri-Omrani, R. Khoder, H. Korri-Youssoufi, Electrochemical functionalization of polypyrrole through amine oxidation of poly(amidoamine) dendrimers: Application to DNA biosensor, Talanta. 154 (2016) 446–454. doi:10.1016/j.talanta.2016.03.076.
[50] T.-M. Wu, H.-L. Chang, Y.-W. Lin, Synthesis and characterization of conductive polypyrrole with improved conductivity and processability, Polym. Int. 58 (2009) 1065–1070. doi:10.1002/pi.2634.
[51] A. Fakhry, F. Pillier, C. Debiemme-Chouvy, Templateless electrogeneration of polypyrrole nanostructures: impact of the anionic composition and pH of the monomer solution, J. Mater. Chem. A. 2 (2014) 9859–9865. doi:10.1039/C4TA01360C.
[52] E. Laviron, General expression of the linear potential sweep voltammogram in the case of diffusionless electrochemical systems, J. Electroanal. Chem. Interfacial Electrochem. 101 (1979) 19–28. doi:10.1016/S0022-0728(79)80075-3.
[53] J.F. Smalley, H.O. Finklea, C.E.D. Chidsey, M.R. Linford, S.E. Creager, J.P. Ferraris, K. Chalfant, T. Zawodzinski, S.W. Feldberg, M.D. Newton, Heterogeneous Electron-Transfer Kinetics for Ruthenium and Ferrocene Redox Moieties through Alkanethiol Monolayers on Gold, J. Am. Chem. Soc. 125 (2003) 2004–2013. doi:10.1021/ja028458j.
[54] E.C. Landis, R.J. Hamers, Covalent Grafting of Ferrocene to Vertically Aligned Carbon Nanofibers: Electron-transfer Processes at Nanostructured Electrodes, J. Phys. Chem. C. 112 (2008) 16910–16918. doi:10.1021/jp806173d.
[55] D. Bao, B. Millare, W. Xia, B.G. Steyer, A.A. Gerasimenko, A. Ferreira, A. Contreras, V.I. Vullev, Electrochemical Oxidation of Ferrocene: A Strong Dependence on the Concentration of the Supporting Electrolyte for Nonpolar Solvents, J. Phys. Chem. A. 113 (2009) 1259–1267. doi:10.1021/jp809105f.
[56] A. Miodek, N. Mejri-Omrani, R. Khoder, H. Korri-Youssoufi, Electrochemical functionalization of polypyrrole through amine oxidation of poly(amidoamine) dendrimers: Application to DNA biosensor, Talanta. 154 (2016) 446–454. doi:10.1016/j.talanta.2016.03.076.
[57] A. Miodek, G. Castillo, T. Hianik, H. Korri-Youssoufi, Electrochemical aptasensor of cellular prion protein based on modified polypyrrole with redox dendrimers, Biosens. Bioelectron. 56 (2014) 104–111. doi:10.1016/j.bios.2013.12.051.
[58] R.M. Elder, J. Pfaendtner, A. Jayaraman, Effect of Hydrophobic and Hydrophilic Surfaces on the Stability of Double-Stranded DNA, Biomacromolecules. 16 (2015) 1862–1869. doi:10.1021/acs.biomac.5b00469.
[59] E. Torres-Chavolla, E.C. Alocilja, Nanoparticle based DNA biosensor for tuberculosis detection using thermophilic helicase-dependent isothermal amplification, Biosens. Bioelectron. 26 (2011) 4614–4618. doi:10.1016/j.bios.2011.04.055.
[60] M. Das, C. Dhand, G. Sumana, A.K. Srivastava, N. Vijayan, R. Nagarajan, B.D. Malhotra, Zirconia grafted carbon nanotubes based biosensor for *M. Tuberculosis* detection, Appl. Phys. Lett. 99 (2011) 143702. doi:10.1063/1.3645618.
[61] C. Liu, D. Jiang, G. Xiang, L. Liu, F. Liu, X. Pu, An electrochemical DNA biosensor for the detection of Mycobacterium tuberculosis, based on signal amplification of graphene and a gold nanoparticle–polyaniline nanocomposite, The Analyst. 139 (2014) 5460–5465. doi:10.1039/C4AN00976B.
[62] C. Thiruppathiraja, S. Kamatchiammal, P. Adaikkappan, D.J. Santhosh, M. Alagar, Specific detection of Mycobacterium sp. genomic DNA using dual labeled gold nanoparticle based electrochemical biosensor, Anal. Biochem. 417 (2011) 73–79. doi:10.1016/j.ab.2011.05.034.

[63] N. Prabhakar, H. Singh, B.D. Malhotra, Nucleic acid immobilized polypyrrole–polyvinylsulphonate film for Mycobacterium tuberculosis detection, Electrochem. Commun. 10 (2008) 821–826. doi:10.1016/j.elecom.2008.03.006.
[64] M. Haddaoui, C. Sola, N. Raouafi, H. Korri-Youssoufi, E-DNA detection of rpoB gene resistance in Mycobacterium tuberculosis in real samples using Fe3O4/polypyrrole nanocomposite, Biosens. Bioelectron. 128 (2019) 76–82. doi:10.1016/j.bios.2018.11.045.